Directed paths in a complex random potential: effects of long-range correlations of the disorder

1992 J. Phys. A: Math. Gen. 25 6517

(http://iopscience.iop.org/0305-4470/25/24/007)

J. Phys. A: Math. Gen. 25 (1992) 6517–6537. Printed in the UK

Directed paths in a complex random potential: effects of long-range correlations of the disorder

Thomas Blum and Yadin Y Goldschmidt

Department of Physics and Astronomy, University of Pittsburgh, Pittsburgh, PA 15260, USA

Received 25 June 1992, in final form 24 August 1992

Abstract. We apply the replica method supplemented by a variational approach to directed paths which acquire random amplitudes and random phases. This problem is pertinent to the hopping of electrons in disordered materials in the variable-range-hopping regime. Here we consider the 'long-range' case in which both the amplitude and phase correlations of the disorder are long-ranged and a mixed case in which amplitude correlations are long-ranged and phase correlations are short-ranged. The variational approach is expected to become exact in the limit of infinite dimensions, and it yields the 'Flory' exponents for the transverse fluctuations. Stationary solutions which extremize the free energy and are characterized by non-trivial patterns of replica-symmetry breaking are obtained both analytically and numerically. The mixed case has a non-trivial phase diagram marked by abrupt changes in the pattern of replica-symmetry breaking. In this case the imaginary part of the random potential plays an important role.

1. Introduction

Recently many investigations have probed the importance of interference effects to the hopping mechanism of conductivity in disordered insulators and semiconductors [1–5]. Interference among the various Feynman paths associated with the motion of electrons through a disordered material can lead to phenomena such as negative magnetoresistance [1–6]. In the weakly localized regime, interference between time-reversed paths (backscattering) plays a crucial role [6]. In the strongly localized regime, on the other hand, long paths do not make a significant contribution, and forwardscattering must be the important interference mechanism. In variable-range hopping, an electron 'hops' to a distant impurity site, and the transmission amplitude for the hop can be viewed as a superposition of virtual paths through the intervening (random) impurity sites [2–5]. When the impurity states are strongly localized, the dominant contribution to the transmission amplitude comes from the shortest paths—those 'directly' connecting the initial and final sites of the hop. In this work, we consider some properties of directed paths which acquire both random phases and random amplitudes. The properties of such walks have arisen in calculations of the localization length [2, 3] and the field-dependence of the magnetoconductance [2, 3, 4b] in disordered insulators.

Another intriguing aspect of these directed paths in random media concerns their relation to spin glasses [7–10]. For instance, Derrida and Spohn [8] have found a mapping between directed walks accumulating random amplitudes (directed

0305-4470/92/246517+21$07.50

polymers) on a Cayley tree and the random energy model, which is in some sense 'the simplest spin glass' [11]. Mézard and Parisi [9] have furthered this connection by applying the replica method to the general case of random manifolds in disordered media. The replica approach facilitates the appropriate averaging over the quenched random variables by introducing copies (replicas) of the system [12]. Mézard and Parisi [9] have explicitly demonstrated the occurrence of replica-symmetry breaking (RSB) (a property first found in the mean-field theory of spin glasses [12]) for random manifolds when the number of embedding dimensions is large. They have attained this result by extending a variational approach originally applied by Shakhnovich and Gutin [13] to the protein-folding problem. The pattern of RSB and the critical exponents obtained in [9] depend on the range of correlation of the disorder.

In a previous work [10], we have applied the variational method to the study of directed paths incurring both real and imaginary random weights with short-range correlations. This extension is important for considering electron hopping in a random medium, since the Feynman paths associated with a hop can pick up random phases as well as random amplitudes while passing through the intervening impurity sites [2]. We have uncovered a rich phase diagram with five phases which differ in the amount of interference effects and in the pattern of binding among replicas for the ground-state wavefunctions. It is tempting to identify one of the phase transitions occurring in that model as the mean-field version of the 'sign transition' proposed by Nguyen, Spivak and Shklovskii [3] to explain changes in the flux periodicity (from h/e to $h/2e$) of the Aharonov–Bohm oscillations as a function of disorder. This identification is based on the common lore that the sign transition coincides with the 'pairing' transition which is named for the formation of tightly bound (replica) pairs in the replica formulation. (The actual occurrence of this transition in the physically relevant dimension has been questioned [4a].)

In the present paper, we consider the case of complex weights with 'long-range' correlations of the disorder as well as a mixed case in which the correlations of the random amplitudes are of long range and those of the random phases are of short range. The interest in long-range correlation of the disorder has both a theoretical and an experimental origin. Theoretically, it has been found for the case of random amplitudes (directed polymers) that even in the mean-field approximation (infinitely large number of dimensions), the exponents characterizing the walk are non-classical, as opposed to short-range interactions that yield trivial (classical) exponents in this limit. Thus, in some sense, the mean-field approximation for long-range correlations is more 'realistic' since it provides a more faithful picture of what we expect in low (physical) dimensions. Experimentally, the hopping distance is always finite, and a measure for the range of the correlations of the disorder is given by comparing the correlation length of the randomness to a typical hopping distance. Therefore, in various samples and realizations of disordered systems, the effective range of the correlations may differ. In this context we have to remember that the finiteness of the hopping distance in experimental situations will exclude a sharp phase transition in the thermodynamic sense whenever it is supposed to occur. A smoother version of the transition might be detected though. Our theoretical results distinguish the cases of short- and long-range correlations by the prediction that phase transitions are lacking in the latter case.

When coupled with standard results from path integration, the replica approach to $(N+1)$-dimensional directed paths leads to the study of non-random, N-dimensional, many-body Schrödinger-like equations. For the problem with complex

weights considered here, the resulting system consists of two sets of n 'particles', which can be thought of as having different 'charges'. Averaging over the real part of the weight leads to an attraction between all particles regardless of their charge; while averaging over the imaginary part results in repulsion between similarly charged particles and attraction between oppositely charged particles. The spatial dependence of these interactions corresponds to the correlations among the random variables in the original system. The replica approach eventually requires taking the $n \to 0$ limit of some quantity; in the present study, we examine the $n \to 0$ limit of the ground-state energy of the system.

One characteristic of directed paths in random media is that the 'average' path wanders significantly farther along the axes transverse to the directed axis than does the non-random version [5, 9, 14–18]. The transverse fluctuations in the non-random case are diffusive: $\langle x^2(t) \rangle \propto t$, where t measures the distance along the directed axis; while in the random case, the transverse fluctuations are superdiffusive and scale as: $\overline{\langle x^2(t) \rangle} \propto t^{2\nu}$, (for large t) where $\nu \geqslant \frac{1}{2}$ and where $\overline{f(x)}$ indicates an averaging over realizations of the randomness. There is a proposed scaling relation between the exponent ν (also denoted by ζ in some papers) and the n-dependence of the ground-state energy of the quantum system that emerges from the replica method. If the ground-state energy scales with the number of particles as

$$E_0(n) = -\mathcal{E}_1 n^{\beta_0} + \mathcal{E}_2 n \tag{1.1}$$

where β_0 is the nonlinear exponent, then ν and β_0 are related by [14, 15]

$$\nu = \frac{1 + \beta_0}{2\beta_0}. \tag{1.2}$$

Kardar [14] has used the (exact) result $\beta_0 = 3$ for a one-dimensional system with delta-function attractions [19] and the above scaling relation to infer that $\nu = \frac{2}{3}$ for two-dimensional directed walks acquiring random amplitudes with delta-function correlations. This claim agrees with numerical simulations [16] and renormalization-group calculations [17]. It should be noted that a 'locality' constraint required in the case of complex weights might spoil this scaling relation, as happens in the model with quadratically correlated random phases [18, 20].

In this work, we apply the replica method to directed paths in a complex random potential. Without the luxury of exact results, we consider the properties of the ground-state energy variationally—in a fashion which explicitly allows for RSB [9, 10, 13]. The approach yields exact results in the limit of a large embedding dimension [9]. First we study directed walks accumulating only random amplitudes with long-range correlations; we calculate β_0 within the variational approach and verify the consistency of the scaling relation equation (1.2) using the values for ν previously obtained by Mézard and Parisi. Next we treat the addition of random phases with long-range correlations. We derive the stationary conditions (equations resulting from the variation) and show that β_0 remains unchanged. When one considers instead random phases with short-range correlations (the 'mixed' case), β_0 again retains its random-amplitude-only value. However, in this case, there arises a non-trivial phase diagram, with regions differing in the amount of interference and in the pattern of RSB.

The rest of the paper is organized as follows. In section 2, we describe the model and derive the many-body system that stems from the replicating procedure. Section 3

introduces the variational approach to finding the ground-state energy of that system. In section 4, we apply the variational method to directed walks acquiring random amplitudes with long-range correlations, emphasizing the extraction of the exponent β_0 and testing the scaling relation between it and ν. In section 5, we obtain the stationary conditions for directed paths in a complex random potential and discuss generic features of their solution. Section 6 contains results when both the real and imaginary random weights have long-range correlations, while section 7 covers the mixed case when the real part has long-range correlations and the imaginary part has short-range correlations. Section 8 consists of a review and a discussion. An appendix provides expressions for the eigenvalues of hierarchical matrices which we use as variational parameters throughout this work.

2. The replica approach to directed walks

The superposition of $(N+1)$-dimensional directed paths that begin at $(\mathbf{0},0)$, end at $(\boldsymbol{y},\tau)$ and accumulate random amplitudes and random phases along the way can be represented by the following path integral

$$Z(\boldsymbol{y},\tau)=\int_{(\mathbf{0},0)}^{(\boldsymbol{y},\tau)}\mathcal{D}\boldsymbol{x}\exp\left\{-\int \mathrm{d}t\left[\frac{\kappa_0}{2}\left(\frac{\partial \boldsymbol{x}}{\partial t}\right)^2+\mathrm{i}\gamma\Theta(\boldsymbol{x},t)+\beta V(\boldsymbol{x},t)\right]\right\} \tag{2.1}$$

where $\boldsymbol{x}$ and $\boldsymbol{y}$ are N-dimensional vectors, $\Theta(\boldsymbol{x},t)$ and $V(\boldsymbol{x},t)$ are random variables, and τ denotes the position along the directed (or 'time-like') axis. The first term in the exponential furnishes a line tension associating a weight with the arclength of the path, the $\mathrm{i}\gamma\Theta(\boldsymbol{x},t)$ term supplies random phases, and $\beta V(\boldsymbol{x},t)$ provides random amplitudes. Let the random variables Θ and V have normal distributions with zero means and correlations of the form

$$\begin{aligned}\overline{V(\boldsymbol{x},t)V(\boldsymbol{x}',t')} &= -\delta(t-t')Nf_v\left[\frac{(\boldsymbol{x}-\boldsymbol{x}')^2}{N}\right]\\ \overline{\Theta(\boldsymbol{x},t)\Theta(\boldsymbol{x}',t')} &= -\delta(t-t')Nf_\theta\left[\frac{(\boldsymbol{x}-\boldsymbol{x}')^2}{N}\right]\end{aligned} \tag{2.2}$$

i.e. short-ranged along the directed axis and of a generic form depending on the distance in the perpendicular plane.

We invoke the replica method to average over the quenched random variables, $\Theta(\boldsymbol{x},t)$ and $V(\boldsymbol{x},t)$. Replicating and averaging $\left(Z^*(\boldsymbol{y},\tau)Z(\boldsymbol{y}',\tau)\right)$ yields

$$\begin{aligned}\overline{\left(Z^*Z\right)^n}(\{\boldsymbol{y}_\alpha\},\tau)=\int_{(\{\mathbf{0}\},0)}^{(\{\boldsymbol{y}_a\},\tau)}\mathcal{D}\boldsymbol{x}_1\ldots\mathcal{D}\boldsymbol{x}_{2n}\exp\Bigg\{-\int \mathrm{d}t\Bigg[\frac{\kappa_0}{2}\sum_a\left(\frac{\partial \boldsymbol{x}_a}{\partial t}\right)^2\\ -\frac{\gamma^2}{2}\sum_{a,b}e_a e_b Nf_\theta\left(\frac{1}{N}(\boldsymbol{x}_a-\boldsymbol{x}_b)^2\right)+\frac{\beta^2}{2}\sum_{a,b}Nf_v\left(\frac{1}{N}(\boldsymbol{x}_a-\boldsymbol{x}_b)^2\right)\Bigg]\Bigg\}\end{aligned} \tag{2.3}$$

where

$$e_a=\begin{cases}+1 & \text{if } a=1,\ldots,n\\ -1 & \text{if } a=n+1,\ldots,2n.\end{cases}$$

The 'partition function' $G(\{x_\alpha\},\tau)=\overline{(Z^*Z)^n(\{x_\alpha\},\tau)}$ involves $2n$ replicas: one set of n from the Z^*s, and the other from the Zs. It is real because we have chosen a distribution for $\Theta(x,t)$ which is symmetric about zero. However, examining the hopping probability for a given sample requires calculating $\langle Z^*(x,\tau)Z(x,\tau)\rangle$ (the same x in each Z), which is real and positive independent of the distribution. Likewise, calculating similar averaged quantities within the replica formalism requires that the positions of one set of replicas coincide with those of the other [18]. This 'locality' constraint can play a very important role especially in the case involving only random phases with long-range correlations.

The partition function $G(\{x_\alpha\},\tau)$ satisfies the Schrödinger-like equation

$$\frac{\partial G(\{x_\alpha\},\tau)}{\partial\tau}=-HG(\{x_\alpha\},\tau) \tag{2.4}$$

where

$$H=-\frac{1}{2}\sum_i\sum_a\frac{\partial^2}{\partial x_{ai}^2}-\frac{\gamma^2}{2}\sum_{a,b}e_a e_b N f_\theta\left(\frac{1}{N\kappa_0}(x_a-x_b)^2\right)+\frac{\beta^2}{2}\sum_{a,b}N f_v\left(\frac{1}{N\kappa_0}(x_a-x_b)^2\right) \tag{2.5}$$

where the x_a have been rescaled by $\kappa_0^{-1/2}$. The interactions among the replicas ('particles') originate in the averaging: the random-amplitude averaging produces purely attractive interactions; while the random-phase averaging furnishes 'charge-dependent' interactions. One can expand the partition function G as

$$G(\{x_\alpha\},\tau)\propto\sum_i\Psi_i^*(\{0\})\Psi_i(\{x_a\})\mathrm{e}^{-E_i\tau} \tag{2.6}$$

where Ψ_i are the eigenstates of H and E_i are the corresponding eigenvalues. The 'free-energy' density of the walk, f, is given by

$$f=\lim_{\tau\to\infty}\lim_{n\to0}\left\{-\frac{1}{\tau n}\ln\left[\int \mathrm{d}x_1\ldots\mathrm{d}x_n\,G(x_1,\ldots,x_n;x_1,\ldots,x_n:\tau)\right]\right\}=\lim_{n\to0}\frac{E_0}{n} \tag{2.7}$$

when $\beta_0>1$ (recall β_0 is the nonlinear exponent in equation (1.1)). When $\beta_0<1$ the above expression diverges. One might consider extending this definition to cases with $\beta_0<1$ by using for f the coefficient of the linear term in equation (1.1).

3. The variational approach

We can extract information on the directed walks such as the scaling of the transverse fluctuations from the ground-state energy of H (equation (2.5))—in particular, from its scaling with n, the number of particles. Since the exact ground-state energy for a generic n-body Hamiltonian is not known, we adopt a variational approach. We choose the following variational wavefunction

$$\Psi=\mathcal{N}\exp\left\{-\frac{1}{2}\sum_{a,b}\sum_{i=1}^{N}\hat{m}_{a,b}x_{ia}x_{ib}\right\} \tag{3.1}$$

where $\hat{m}$ is a $2n \times 2n$ matrix containing variational parameters. A Gaussian wavefunction is selected primarily for calculational facilitation. Because of the eventual continuation to $n \to 0$, one should not only be able to compute the expectation energy for general n but also allow for the possibility of replica-symmetry breaking that might arise in the $n \to 0$ limit. This Gaussian-variational approach produces the exact ground-state energy in the limit of large embedding dimension (large N) [9]. Note that Ψ is the exact ground state of the following Hamiltonian

$$h = -\frac{1}{2}\sum_{i=1}^{N}\sum_{a}\frac{\partial^2}{\partial x_{ia}^2} + \frac{1}{2}\sum_{i=1}^{N}\sum_{a,b}\hat{M}_{a,b}x_{ia}x_{ib} \tag{3.2}$$

where $\hat{m}$ and $\hat{M}$ are related by

$$\hat{m} = (\hat{M})^{1/2}. \tag{3.3}$$

Some physical intuition may be obtained by considering h as a variational approximation to H with variational parameters representing effective 'interactions' among replicas. One should note, however, that not all properties of H are necessarily reproduced in h. For instance, the ground-state energies of H and h do not coincide, even when Ψ yields the exact ground-state energy of H as is the case for $N \to \infty$. See equations (3.5) and (3.6) below.

With the Gaussian wavefunction, calculating $\langle H\rangle_\Psi$ requires computing $\mathrm{Tr}(\hat{m})$ and $(m_{a,a}^{-1} + m_{b,b}^{-1} - 2m_{a,b}^{-1})$. The trace arises from the expectation of the kinetic-energy portion of H; the other quantity emerges from the interaction terms. In particular, a Taylor expansion and Wick's theorem applied to an interaction term yield

$$\left\langle f\left[\frac{(x_a - x_b)^2}{\kappa_0 N}\right]\right\rangle_\Psi = \sum_j \frac{f^{(j)}}{j!\kappa_0^j N^j}\left\langle (x_a - x_b)^{2j}\right\rangle_\Psi$$

$$= \sum_j \frac{f^{(j)}}{j!\kappa_0^j N^j}\,\frac{(N+2j-2)!!}{(N-2)!!}\,\frac{\left(m_{a,a}^{-1} + m_{b,b}^{-1} - 2m_{a,b}^{-1}\right)^j}{2^j}$$

$$= \hat{f}\left[\frac{m_{a,a}^{-1} + m_{b,b}^{-1} - 2m_{a,b}^{-1}}{2\kappa_0}\right] \tag{3.4a}$$

where

$$\hat{f}(x) = \frac{1}{\Gamma(N/2)}\int_0^\infty \mathrm{d}\alpha\, \alpha^{\frac{N}{2}-1}\mathrm{e}^{-\alpha} f\left(\frac{2\alpha x}{N}\right). \tag{3.4b}$$

If the correlations have long-range behaviour, i.e. $f(x) \propto x^{1-\gamma_0}$, then $\hat{f}$ scales in the same way as f, i.e. $\hat{f}(x) \propto x^{1-\gamma_0}$, provided $\gamma_0 \leqslant \frac{N}{2} + 1$ [9].

The expectation of the Hamiltonian (2.5) with the wavefunction (3.1) becomes

$$\frac{1}{N}\langle H\rangle_\Psi = \frac{1}{2}\sum_a m_{aa} - \frac{\gamma^2}{2}\sum_{a,b} e_a e_b \hat{f}_\theta\left[\frac{m_{aa}^{-1} + m_{bb}^{-1} - 2m_{ab}^{-1}}{2\kappa_0}\right]$$

$$+ \frac{\beta^2}{2}\sum_{a,b}\hat{f}_v\left[\frac{m_{aa}^{-1} + m_{bb}^{-1} - 2m_{ab}^{-1}}{2\kappa_0}\right]. \tag{3.5}$$

Note for comparison that the ground-state energy of h (equation (3.2)) is given by

$$\frac{1}{N}E_h^0 = \sum_a m_{aa}. \tag{3.6}$$

The energy in (3.6) differs from (3.5) even for the 'best' variational matrix m_{ab}. This difference is a well-known feature of mean-field theory. For a similar phenomenon in the Lagrangian formalism, see [9, equation (III.5)].

Just as the Gaussian form of the wavefunction is selected mainly for computational reasons, so too is the form of the matrix $\hat{M}$ chosen with the eventual $n \to 0$ continuation in mind. Our parametrization scheme first breaks the $2n \times 2n$ matrix $\hat{M}$ into two $n \times n$ matrices as follows

$$\hat{M} = \begin{pmatrix} \hat{\Sigma}_1 & \hat{\Sigma}_2 \\ \hat{\Sigma}_2 & \hat{\Sigma}_1 \end{pmatrix} \tag{3.7}$$

with $\hat{\Sigma}_1$ denoting interactions among equally charged particles and $\hat{\Sigma}_2$ interactions among oppositely charged particles. We have chosen both Σs to be hierarchical matrices as introduced by Parisi [12]. Each hierarchical matrix $\hat{\Sigma}$ consists of a set of variational parameters $(\tilde{\sigma}, \sigma_0, \sigma_1, \ldots, \sigma_K)$ and is designed so that quantities calculated from it have a well-defined $n \to 0$ limit. After the limit, such quantities involve $\tilde{\sigma}$ and a function $\sigma(u)$ on the interval $[0,1]$. Hierarchical matrices are readily diagonalized and have an equal number of variational parameters and distinct eigenvalues. We find it convenient to vary the matrix elements of the $\hat{\Sigma}$s with respect to the eigenvalues of $\hat{m}$ instead of the original interaction parameters. See the appendix for relationships between the matrix elements and the eigenvalues.

4. Random amplitudes

In this section we briefly consider directed walks which acquire just random amplitudes. The reason for doing so is twofold: (1) to provide a synopsis of Mézard and Parisi's contribution and (2) to derive an expression for the n-dependent ground-state energy which is not found in that work. The latter enables us to obtain the exponent β_0 directly and then to verify the scaling relation (equation (1.2)). Averaging solely over real weights requires only one set of n replicas and leads to the following Hamiltonian

$$H = -\frac{1}{2}\sum_i \sum_a \frac{\partial^2}{\partial x_{ai}^2} + \frac{\beta^2}{2}\sum_{a,b} N f_v\left(\frac{1}{N\kappa_0}(\boldsymbol{x}_a - \boldsymbol{x}_b)^2\right) \tag{4.1}$$

with all interactions attractive. We calculate the expectation of this Hamiltonian with respect to Ψ (equation (3.1)) in which $\hat{m}$ is a single $n \times n$ hierarchical matrix with K-step breaking in the limits $K \to \infty$ and $n \to 0$. We use the eigenvalues of $\hat{m}$ as the variational parameters; after the limits are taken, the eigenvalues take the form of $(\tilde{\lambda}, \lambda(u))$, where $\lambda(u)$ is a function on the interval $[n,1]$. (See the appendix.) We choose to retain n instead of replacing it by zero (as is more customary), since we intend to find the n-dependence of the ground-state energy.

Calculating $\langle H\rangle_\Psi$ leads to the following expression

$$\frac{\langle H\rangle_\Psi}{Nn} = \frac{1}{4}\int_1^n \frac{du}{u^2}\lambda(u) + \frac{1}{4n}\tilde{\lambda} + \frac{\beta^2}{2}\int_1^n du\, \hat{f}[Q(u)] \tag{4.2a}$$

where

$$\kappa_0 Q(u) = \int_1^u \frac{dv}{v^2}\lambda^{-1}(v) + \frac{1}{u}\lambda^{-1}(u). \tag{4.2b}$$

The first two terms in $\langle H\rangle_\Psi/Nn$ constitute the kinetic-energy portion, which is simply the trace of $\hat{m}$. The third term arises from the interactions, where $Q(u)$ represents $[m_{a,a}^{-1} + m_{b,b}^{-1} - 2m_{a,b}^{-1}]/2\kappa_0$. (See equation (3.5).) The eigenvalue $\tilde{\lambda}$ is associated with the centre-of-mass mode and has a multiplicity of one. Note that the other eigenvalues $\lambda(u)$ have multiplicities $n\,du/u^2$ in the continuum limit (see equation (A.4) in the appendix) which occurs in the expression above wherever $\lambda(u)$ does, i.e. in the kinetic-energy term and within $Q(u)$—the argument of $\hat{f}$—but not in the integration over $\hat{f}$.

Varying $\langle H\rangle_\Psi/Nn$ with respect to $\tilde{\lambda}$ leads to $\tilde{\lambda} = 0$, which is simply the usual result of translational invariance. Taking a functional derivative of equation (4.2) with respect to $\lambda(u)$ and setting it equal to zero yields

$$\kappa_0\lambda^2(u) = 2\beta^2\left\{\int_u^n dv\, \hat{f}'[Q(v)] + u\hat{f}'[Q(u)]\right\}. \tag{4.3}$$

(Note that $\lambda^2(u)$ corresponds to $[\sigma](u)$ in the notation of Mézard and Parisi.) We assume the following form for the 'long-range' correlations

$$\lim_{x\gg 1}\hat{f}(x) = \left(\frac{1}{1-\gamma_0}\right)x^{(1-\gamma_0)}. \tag{4.4}$$

If $\gamma_0 < 2$ the large-x behaviour dominates and no regularization is necessary for small x; consequently, the above expression can and will be used for all x. The coefficient $(1/1-\gamma_0)$ is chosen such that the interactions remain attractive. A few derivatives with respect to u and some algebra can eliminate the integrals from the stationary equation (equation (4.3)) and produce the following local expression

$$[\kappa_0^{\gamma_0-1}\beta^2\gamma_0]^{1/1+\gamma_0}\left[\frac{3u}{1+\gamma_0}\right]\lambda'(u) = \lambda^{(2-\gamma_0)/(1+\gamma_0)}(u)\lambda'(u). \tag{4.5}$$

Note that this equation has two solutions, one of which is $\lambda'(u) = 0$ (i.e. $\lambda(u) =$ constant) and the second is a simple power of u: $\lambda(u) = Au^\alpha$. Returning to the integral form to connect these two solutions, one determines

$$\lambda(u) = \begin{cases} \Lambda_0\left[\dfrac{3u}{1+\gamma_0}\right]^{(1+\gamma_0)/(2-\gamma_0)} & \text{if } n < u < \frac{1+\gamma_0}{3} \\ \Lambda_0 & \text{if } \frac{1+\gamma_0}{3} < u < 1 \end{cases} \tag{4.6}$$

where $\Lambda_0 = [\kappa_0^{\gamma_0-1}\beta^2\gamma_0]^{1/2-\gamma_0}$. The two solutions meet at $u_c = (1+\gamma_0)/3$, independent of β, the 'strength' of of the random amplitudes. As a result, the

pattern of RSB does not change with β and no phase transition occurs in this model. There also exist finite-step breaking solutions to the stationary equation in which $\lambda(u)$ is piecewise constant on intervals; however, such solutions do not represent the 'best' variational solution.

Substituting the solution (equation (4.6)) into $\langle H\rangle_\Psi$ (equation (4.2)) gives rise to

$$\langle H\rangle_\Psi(n,\gamma_0) = \frac{N(2-\gamma_0)^2\Lambda_0}{4(1-2\gamma_0)(1-\gamma_0)}\left\{2n - \frac{(1+7\gamma_0)}{9\gamma_0}\left(\frac{3n}{1+\gamma_0}\right)^{(1+\gamma_0)/(2-\gamma_0)}\right\} \tag{4.7}$$

from which one can deduce

$$\beta_0 = \frac{1+\gamma_0}{2-\gamma_0}. \tag{4.8}$$

Using this expression and the scaling relation (equation (1.2)), one finds for ν, the exponent associated with the transverse fluctuations

$$\nu = \frac{3}{2(1+\gamma_0)} \tag{4.9}$$

which agrees with the 'Flory' exponents [9, 22]. Note, however, that equations (4.2) and (4.7) for the ground-state energy differ from the free-energy density provided in equation (5.5) of [9]. Their free-energy density corresponds to the $n \to 0$ limit of $\langle H\rangle_\Psi/n$ which can be taken only for $\beta_0 > 1$ ($\gamma_0 > \frac{1}{2}$) and is given by the coefficient of the linear term in n in equation (4.7).

The expression for $\langle H\rangle_\Psi(n,\gamma_0)$ diverges at $\gamma_0 = 0$, $\frac{1}{2}$, and 1; while that for β_0 diverges at $\gamma_0 = 2$. The RSB solution (equation (4.6)) is trivial when $\gamma_0 = 0$ since $\Lambda_0 = 0$. The right solution is the replica symmetric one [21], but β_0 and ν are still given correctly by equations (4.8) and (4.9). The divergence at $\gamma_0 = \frac{1}{2}$ marks the point at which the nonlinear exponent β_0 becomes linear and where $\nu = 1$, indicating that the transverse fluctuations are ballistic. The divergence at $\gamma_0 = 1$ is attributable to the choice of $(1/1-\gamma_0)$ as the coefficient of the correlations and can be eliminated by using instead $\mathrm{sign}(1-\gamma_0)$ (with $\mathrm{sign}(0) = -1$). In this case, the interactions have no spatial dependence and $\langle H\rangle$ is proportional to $\frac{1}{2}n(n-1)$, the number of interactions [15]. Note that both the $\gamma_0 = 0$ and $\gamma_0 = 1$ solutions are dimension-independent, implying that the Flory exponents (found in infinite dimensions) apply in all dimensions. There are some speculations [22, 23] that there is a range of γ_0 values for which the exponents are dimension-independent, but it is certainly not the case for all values of γ_0. Consider, for example, the case of $\gamma_0 = \frac{3}{2}$, corresponding to an $\hat{f}(x)$ which scales in the same fashion as a one-dimensional delta function. The Flory exponents in this case are $\beta_0 = 5$ and $\nu = \frac{3}{5}$; whereas the exact exponents for two-dimensional directed polymers with delta-function correlations are $\beta_0 = 3$ and $\nu = \frac{2}{3}$ [14, 16, 17]. Finally, the divergence of β_0 at $\gamma_0 = 2$ marks the onset of short-range behaviour and a return to diffusive transverse fluctuations.

5. Random amplitudes and random phases

Next we address walks in a complex random potential. Recall that in this case we have chosen as the variational matrix a 2×2 matrix of $n \times n$ hierarchical matrices.

Provided the two $n \times n$ matrices commute (which is the case for matrices with the same pattern of breaking and is certainly the case in the limit of full breaking), the eigenvalues of the $2n \times 2n$ are the sum and the difference of eigenvalues of the $n \times n$ matrices; hence, we call them $(\bar{\lambda}_+, \lambda_+(u))$ and $(\bar{\lambda}_-, \lambda_-(u))$.

The expectation of H (equation (2.5)) with respect to Ψ (equation (3.1)) yields

$$\frac{\langle H\rangle_\Psi}{Nn} = \frac{1}{4}\int_1^n \frac{\mathrm{d}u}{u^2}\left(\lambda_+(u)+\lambda_-(u)\right) + \frac{1}{4n}\left(\bar{\lambda}_+ + \bar{\lambda}_-\right)$$
$$+ \beta^2\left\{\int_1^n \mathrm{d}u\, \hat{f}_v[R(u)] + \int_1^n \mathrm{d}u\, \hat{f}_v[T+S(u)] + \hat{f}_v[T]\right\}$$
$$+ \gamma^2\left\{-\int_1^n \mathrm{d}u\, \hat{f}_\theta[R(u)] + \int_1^n \mathrm{d}u\, \hat{f}_\theta[T+S(u)] + \hat{f}_\theta[T]\right\} \qquad (5.1a)$$

where

$$\kappa_0 R(u) = \frac{1}{2}\int_1^u \frac{\mathrm{d}v}{v^2}\left(\lambda_+^{-1}(v)+\lambda_-^{-1}(v)\right) + \frac{1}{2u}\left(\lambda_+^{-1}(u)+\lambda_-^{-1}(u)\right) \qquad (5.1b)$$

$$\kappa_0 S(u) = \frac{1}{2}\int_1^u \frac{\mathrm{d}v}{v^2}\left(\lambda_+^{-1}(v)-\lambda_-^{-1}(v)\right) + \frac{1}{2u}\left(\lambda_+^{-1}(u)-\lambda_-^{-1}(u)\right) \qquad (5.1c)$$

and

$$\kappa_0 T = \int_1^n \frac{\mathrm{d}v}{v^2}\lambda_-^{-1}(v) + \frac{1}{n}\bar{\lambda}_-^{-1}. \qquad (5.1d)$$

The first line in equation (5.1*a*) arises from the kinetic energy (and is just the trace of $\hat{m}$); the second and third lines come from the interaction terms, with the R terms corresponding to interactions among similarly charged particles and the T and $(T+S)$ terms representing those among oppositely charged particles.

Functional derivatives of $\langle H\rangle_\Psi/Nn$ lead to the following (coupled) stationary equations

$$\kappa_0\lambda_+^2(u) = 2\beta^2\left\{\int_u^n \mathrm{d}v\left(\hat{f}_v'[R(v)] + \hat{f}_v'[T+S(v)]\right)\right.$$
$$\left. + u\left(\hat{f}_v'[R(u)] + \hat{f}_v'[T+S(u)]\right)\right\}$$
$$- 2\gamma^2\left\{\int_u^n \mathrm{d}v\left(\hat{f}_\theta'[R(v)] - \hat{f}_\theta'[T+S(v)]\right)\right.$$
$$\left. + u\left(\hat{f}_\theta'[R(u)] - \hat{f}_\theta'[T+S(u)]\right)\right\}$$

and

$$\begin{aligned}\kappa_0\lambda_-^2(u) = 2\beta^2\Big\{&\int_u^n \mathrm{d}v\left(\hat{f}_v'[R(v)] - \hat{f}_v'[T+S(v)]\right)\\ &+ u\left(\hat{f}_v'[R(u)] - \hat{f}_v'[T+S(u)]\right)\Big\}\\ &+ 4\beta^2\Big\{\int_1^n \mathrm{d}v\,\hat{f}_v'[T+S(v)] + \hat{f}_v'[T]\Big\}\\ &- 2\gamma^2\Big\{\int_u^n \mathrm{d}v\left(\hat{f}_\theta'[R(v)] + \hat{f}_\theta'[T+S(v)]\right)\\ &+ u\left(\hat{f}_\theta'[R(u)] + f_\theta'[T+S(u)]\right)\Big\}\\ &+ 4\gamma^2\Big\{\int_1^n \mathrm{d}v\,\hat{f}_\theta'[T+S(v)] + \hat{f}_\theta'[T]\Big\}. \end{aligned} \tag{5.2}$$

Variation with respect to $\bar{\lambda}_+$ yields $\bar{\lambda}_+ = 0$ (which is simply a consequence of translational invariance). Variation with respect to $\bar{\lambda}_-$ produces a third stationary equation; however, except in the case of $\gamma_0 = 0$ (quadratically correlated disorder), $\bar{\lambda}_-$ ends up equaling $\lim_{n\to 0}\lambda_-(n)$.

In a previous work [10], we have considered a model with short-range correlations of the form

$$\hat{f}_v(x) = \hat{f}_\theta(x) = \begin{cases} f_0 + f_1 x & \text{if } 0 \leqslant x \leqslant |f_0|/f_1 \\ 0 & \text{otherwise} \end{cases} \tag{5.3}$$

where f_0 is negative. For $\beta > \sqrt{2}$ and $\gamma < \sqrt{\frac{3}{2}}$ (which lies within what is called phase II in [10]), we have found a solution with one-step breaking of the following form

$$\begin{aligned}\lambda_+(u) &= \begin{cases} 0 & \text{if } n < u < k \\ 2k^{1/2} f_1^{1/2}\beta/\kappa_0^{1/2} & \text{if } k < u < 1 \end{cases}\\ \lambda_-(u) &= \begin{cases} 2k^{1/2} f_1^{1/2}(\beta^2+\gamma^2)^{1/2}/\kappa_0^{1/2} & \text{if } n < u < k \\ 2k^{1/2} f_1^{1/2}\beta/\kappa_0^{1/2} & \text{if } k < u < 1 \end{cases}\end{aligned} \tag{5.4a}$$

where

$$-4k^{3/2}\beta^2\left(\frac{|f_0|\kappa_0^{1/2}}{f_1^{1/2}}\right) + (2k+2)\beta = (\beta^2+\gamma^2)^{1/2}. \tag{5.4b}$$

In the short-range version, the pattern of RSB (e.g. the value of k) depends on the parameters β and γ, and five phases have been found.

Certain features seen in the short-range solutions carry over to the 'long-range' solutions. In fact, to some extent, the latter represents a 'smoothing out' of the former. For example, the long-range $\lambda_+(u)$ does not equal zero but rather approaches it as

$u \to 0$. One can understand this feature by first noting that $[\lambda_+(n) - \tilde{\lambda}_+] \propto n$ (as can be shown from equation (A.5) in the appendix) and then recalling that $\tilde{\lambda}_+ = 0$; combining these results implies $\lambda_+(n) \to 0$ in the $n \to 0$ limit. At the other endpoint ($u = 1$), the long-range $\lambda_+(u)$ approaches a constant, as does $\lambda_-(u)$ at both endpoints. Moreover, in both the short- and long-range versions, these constants are observed to obey the following inequality

$$\lambda_+(1) \leqslant \lambda_-(1) \leqslant \lambda_-(0). \tag{5.5}$$

We have noted in the short-range model that the above relation is a consequence of a stronger attraction between oppositely charged particles than between similarly charged particles [10].

6. The long-range case

In this section, we consider walks in which the real and imaginary random potentials have long-range correlations of the form

$$f_v(x) = f_\theta(x) = \left(\frac{1}{1-\gamma_0}\right) x^{(1-\gamma_0)}. \tag{6.1}$$

We could not find a complete analytic solution to the stationary equations for general β, γ and γ_0; however, we could solve them in a few special instances. The case of quadratically correlated disorder ($\gamma_0 = 0$) was first solved for a real potential [21] and then for a purely imaginary potential [18, 20, 24]. We have found that even for the general complex potential case given by (6.1) the Hamiltonian is diagonalizable and the eigenvalues of $\hat{m}$, the matrix associated with Ψ (equation (3.1)), are

$$\begin{aligned} \lambda_+(u) &= \lambda_-(u) \equiv 2\beta n^{1/2}/\kappa_0^{1/2} \\ \tilde{\lambda}_- &= 2(\beta^2 + \gamma^2)^{1/2} n^{1/2}/\kappa_0^{1/2}. \end{aligned} \tag{6.2}$$

In this case, one has available exact expressions for the ground-state energy and the partition function $G(\{x_\alpha\}, \tau)$ and can calculate β_0 and ν independently. For $\beta = 0$ (random phases only), one finds $\beta_0 = \frac{1}{2}$ and $\nu = \frac{1}{2}$, demonstrating that the scaling relation (eq.(1.2)) does not hold in this instance [18, 20].

One can also solve the stationary equations analytically if the 'strength' of the random phases γ is set to zero, i.e. return to the random-amplitude model solved earlier. The solution changes slightly since the variation now involves two sets of n replicas; it becomes

$$\begin{aligned} \lambda_+(u) &= \begin{cases} \Lambda_0 \left[\dfrac{6u}{1+\gamma_0}\right]^{(1+\gamma_0)/(2-\gamma_0)} & \text{if } n < u < \frac{1+\gamma_0}{6} \\ \Lambda_0 & \text{if } \frac{1+\gamma_0}{6} < u < 1 \end{cases} \\ \lambda_-(u) &\equiv \Lambda_0. \end{aligned} \tag{6.3}$$

Note that in this expression u_c takes half the value it does in the previous solution (equation (4.6)). Another solvable case arises when the strength of the real potential β is set to zero, for which we have found the following replica-symmetric solution

$$\begin{aligned} \lambda_+(u) &\equiv 0 \\ \lambda_-(u) &\equiv (4\gamma^2/\kappa_0^{1+\gamma_0})^{1/2-\gamma_0}. \end{aligned} \tag{6.4}$$

These last two solutions (equations (6.3) and (6.4)) are only valid for $\gamma_0 \neq 0$, and one does not recover the $\gamma_0 = 0$ solution (equation (6.2)) by setting γ_0 to zero.

In addition to solving this select set of examples, one can demonstrate certain analytic properties of the solutions to the stationary equations for general β, γ and γ_0 as well as solve them numerically. A few derivatives with respect to u and a bit of algebra lead to the following local stationary conditions

$$\begin{aligned} &\left[3\lambda_+\lambda_-^3(\lambda_+')^3 \pm 2\lambda_-^4(\lambda_+')^2\lambda_-' \pm \lambda_+\lambda_-^3\lambda_+'(\lambda_-')^2 \right. \\ &\qquad \left. \pm \lambda_+\lambda_-^4\lambda_+'\lambda_-'' \mp \lambda_+^4\lambda_-\lambda_+'\lambda_-'' + \{\lambda_+ \leftrightarrow \lambda_-\}\right] \\ &= \left(\frac{\gamma_0+1}{2u}\right)\frac{[\lambda_+\lambda_+' \pm \lambda_-\lambda_-'][\lambda_-^2\lambda_+' \pm \lambda_+^2\lambda_-']^2}{\lambda_+\lambda_-} \\ &\quad \times \left[\frac{\lambda_+^2\lambda_-^2[\lambda_+\lambda_+' \pm \lambda_-\lambda_-']}{\gamma_0(\beta^2 \mp \gamma^2)[\lambda_-^2\lambda_+' \pm \lambda_+^2\lambda_-']}\right]^{1/1+\gamma_0} \end{aligned} \tag{6.5}$$

where the u-dependence of the λs has been suppressed and κ_0 has been set to one. This expression represents two coupled equations—the first supplied by the upper signs, the second by the lower signs.

Consider an expansion of the λs for small u. Recall that $\lim_{u\to 0}\lambda_+(u) = 0$ and $\lim_{u\to 0}\lambda_-(u) =$ constant and add to each the first correction—some power of u

$$\begin{aligned} \lambda_+(u) &= Au^\alpha + O(u^{3\alpha}) \\ \lambda_-(u) &= B - Cu^\chi + O(u^{2\chi}) \end{aligned} \tag{6.6}$$

and substitute these expressions into equation (6.5). A power-counting argument reveals that

$$\alpha = \frac{1}{2}\chi = \frac{\gamma_0+1}{2-\gamma_0}. \tag{6.7}$$

After extracting the leading power in u and simplifying the expressions, one finds

$$A = \Lambda_0\left[\frac{6}{\gamma_0+1}\right]^{(\gamma_0+1)/(2-\gamma_0)} \tag{6.8}$$

and

$$2BC = \frac{\gamma^2}{\beta^2}A^2. \tag{6.9}$$

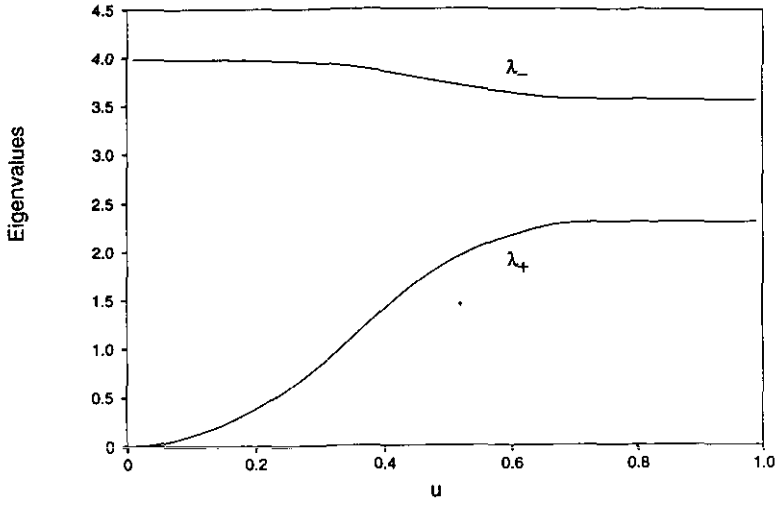

Figure 1. The eigenvalues $\lambda_+(u)$ and $\lambda_-(u)$ for $\gamma_0 = 1$, $\beta = 1.0$, $\gamma = 0.7$ and $\kappa_0 = 1.0$ that arise from numerical calculations in the long-range case.

The various derivatives involved in obtaining the local expression of the stationary equations prevent one from determining the coefficients B and C individually. Note that the small-u behaviour of $\lambda_+(u)$ maintains its $\gamma = 0$ form so long as $\beta \neq 0$. Since the nonlinear exponent β_0 is determined solely by $\lambda_+(u)$ at small u, one can conclude that $\beta_0 = (1+\gamma_0)/(2-\gamma_0)$ and $\nu = 3/2(1+\gamma_0)$ in the long-range case (for $\beta \neq 0$).

In fact, one can construct a reasonable approximate solution by assuming that $\lambda_+(u)$ preserves its $\gamma = 0$ form but that u_c acquires some γ-dependence and that $\lambda_-(u)$ develops a break at u_c, equaling one constant below u_c and another constant above u_c (with the difference being some function of γ). The actual shape is smoother but functionally more complicated. A more complete characterization of $\lambda_+(u)$ and $\lambda_-(u)$ is readily gained through a numerical solution to the integral version of the stationary equations. To this end, we have simply iterated equations (5.2), using as a starting point functions which roughly approximate $\lambda_+(u)$ and $\lambda_-(u)$ in the $\gamma = 0$ solution (equation (6.3)). Figure 1 shows one such solution. The relations found above concerning the small u behaviour have been confirmed numerically. For this long-range model, we have discerned no numerical evidence for abrupt changes in the pattern of RSB of the sort that occurred in the short-range version, that is, we have seen no manifestation of a phase transition (except at $\beta = 0$ where the RS solution is recovered).

Unlike what happens in the short-range model, the solutions in the long-range case exhibit signs of interference effects for even the smallest γ. One of the order parameters useful in characterizing the phases uncovered in the short-range model is σ_d which is the 'additional' variable along the diagonal of $\hat{\Sigma}_2$, the matrix parametrizing the interactions among oppositely charged particles [10]. It measures the tendency for pairing of replicas. In terms of the eigenvalues, it is expressed as

$$\sigma_d = \frac{1}{2}(\lambda_-^2(1) - \lambda_+^2(1)). \tag{6.10}$$

In the short-range model, $\sigma_d = 0$ in three of the five phases; whereas, every solution found in the long-range model (with the exception of those for $\gamma = 0$ and $\gamma_0 = 0$) has non-zero σ_d.

7. Mixed case

Now let us discuss the case in which the phase correlations are short-ranged while the amplitude correlations are long-ranged

$$\hat{f}_\theta(x) = \begin{cases} f_{\theta 0} + f_{\theta 1} x & \text{if } 0 \leqslant x \leqslant |f_{\theta 0}|/f_{\theta 1} \\ 0 & \text{otherwise} \end{cases}$$
$$f_v(x) = \left(\frac{1}{1-\gamma_0}\right) x^{(1-\gamma_0)}. \tag{7.1}$$

Such a model will have non-trivial exponents β_0 and ν (as does the long-range version) and a non-trivial phase diagram (as does the short-range version). One can envisage a real system for which amplitude correlations among random scatterers are long-ranged, while phase coherence is short-ranged.

For $\gamma = 0$, one recovers the solution provided in equation (6.3). Since $\hat{f}_\theta(x)$ is non-zero only for a finite range of arguments, the $\gamma = 0$ solution remains valid for non-zero γ provided all of the arguments of $\hat{f}_\theta$ lie outside this range. This condition is met when

$$\min[R(u)] = \min[T + S(u)] = T \geqslant \frac{|f_{\theta 0}|}{f_{\theta 1}} \tag{7.2}$$

which in turn implies

$$\beta \leqslant \gamma_0^{-1/2} \kappa_0^{-1/2} \left[\frac{|f_{\theta 0}|}{f_{\theta 1}}\right]^{(-2+\gamma_0)/2}. \tag{7.3}$$

This condition indicates when equation (6.3) satisfies the stationary equations in the mixed case and not when it represents the 'best' solution. The addition of random phases is irrelevant to this particular solution; consequently, it has no features attributable to interference such as pairing of replicas ($\sigma_d = 0$).

We have been able to find a second analytic solution to the stationary equations in the mixed case

$$\lambda_+(u) = \begin{cases} \Lambda_0 \left[\dfrac{6u}{1+\gamma_0}\right]^{(1+\gamma_0)/(2-\gamma_0)} & \text{if } n < u < u_c \\ \Lambda_0 \left[\dfrac{6u_c}{1+\gamma_0}\right]^{(1+\gamma_0)/(2-\gamma_0)} & \text{if } u_c < u < 1 \end{cases}$$
$$\lambda_-(u) \equiv \Lambda_0 \left[\frac{6u_c}{1+\gamma_0}\right]^{(1+\gamma_0)/(2-\gamma_0)} \left[\frac{3u_c}{1+\gamma_0-3u_c}\right]. \tag{7.4}$$

In this solution, $\lambda_+(u)$ maintains its $\gamma = 0$ form, but u_c becomes γ-dependent. The break point u_c is determined by the following equation

$$\left[\frac{3u_c}{1+\gamma_0-3u_c}\right]^2 = \frac{4}{\gamma_0}\left[\frac{1+\gamma_0}{6u_c}\right]\left\{u_c - 1 - \left[\frac{2-\gamma_0}{2(1+\gamma_0)}\right]u_c + \left[\frac{1+\gamma_0}{2(1+\gamma_0-3u_c)}\right]^{\gamma_0}\right\}$$
$$+ \frac{4\gamma^2}{\kappa_0}\Lambda_0^{-2}\left[\frac{6u_c}{1+\gamma_0}\right]^{-2(1+\gamma_0)/(2-\gamma_0)} \hat{f}_\theta'\left[\frac{\lambda_-^{-1}}{\kappa_0}\right]. \tag{7.5}$$

It turns out that u_c lies between $(1+\gamma_0)/6$ and $(1+\gamma_0)/3$ and approaches the latter for large γ. Note that $\lambda_-(1) \neq \lambda_+(1)$ ($\sigma_d > 0$), indicating that pairing takes place.

Instead of having no contribution from the $\hat{f}_\theta$s as in the previous ($\gamma = 0$) solution, the second solution (equation (7.4)) has one contribution from them. The non-zero term is $\hat{f}_\theta(T)$, which arises from 'pairing' interactions, i.e. terms such as: $\hat{f}_\theta[(m_{i,i}^{-1} + m_{n+i,n+i}^{-1} - 2m_{i,n+i}^{-1})/2\kappa_0]$. Hence, this solution requires that

$$\min[R(u)] = \min[T + S(u)] \geqslant \frac{|f_{\theta 0}|}{f_{\theta 1}} \tag{7.6a}$$

while

$$T \leqslant \frac{|f_{\theta 0}|}{f_{\theta 1}}. \tag{7.6b}$$

Substituting the solution (equation (7.4)) into these conditions yields

$$\beta^2\left(\frac{6u_c}{1+\gamma_0}\right)^3 \leqslant \gamma_0^{-1}\kappa_0^{-1}\left[\frac{|f_{\theta 0}|}{f_{\theta 1}}\right]^{-2+\gamma_0} \tag{7.7a}$$

and

$$\beta^2\left(\frac{6u_c}{1+\gamma_0}\right)^{1+\gamma_0}\left(\frac{3u_c}{1+\gamma_0-3u_c}\right) \geqslant \gamma_0^{-1}\kappa_0^{-1}\left[\frac{|f_{\theta 0}|}{f_{\theta 1}}\right]^{-2+\gamma_0} \tag{7.7b}$$

respectively.

A comparison of ground-state energies (which correspond to 'free energies' of the walks) furnishes the solid phase boundary shown in figure 2. The solution given by equation (6.3) is the better solution in region I of the figure when compared to the solution (7.4) (it has a lower free energy), and the opposite is true in region III of the figure. This provides strong evidence for a phase transition, whose approximate location is given by the solid boundary in figure 2. Although this phase boundary approaches the $\gamma = 0$ axis, there is no phase transition along this axis.

We have found numerically that there exist solutions which extremize the free energy in addition to those given explicitly above. The presence of these other solutions supports the existence of the solid boundary in the figure, but since we are uncertain as to which is really the correct solution we have referred to the phase boundary above as 'approximate'. The numerical solutions also suggest that there might be another phase boundary which separates the low and high β-regions for large γ, as indicated by the dashed line in figure 2. Conditions (7.7*a*) and (7.7*b*)

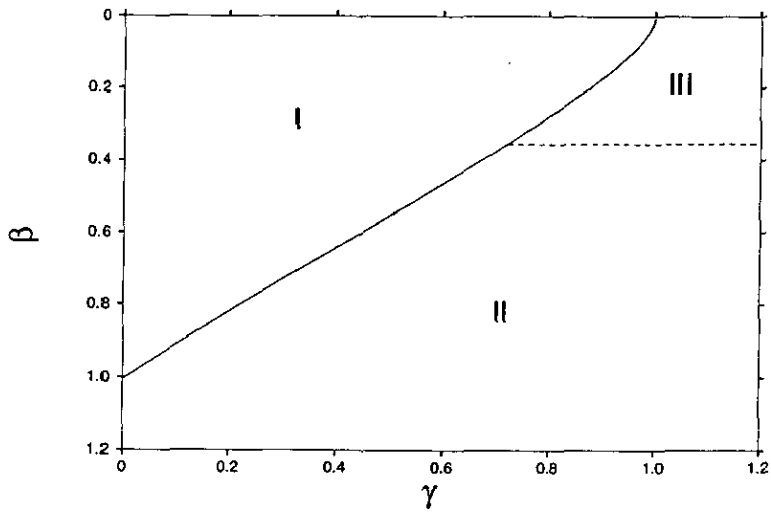

Figure 2. Proposed phase diagram for the mixed case. The solid curve is obtained by equating the free energies for solutions (6.3) and (7.4) for $\gamma_0 = 0.99$, $f_{\theta 0} = -1.0$, $f_{\theta 1} = 1.0$, and $\kappa_0 = 1.0$. The broken line is another likely phase boundary.

restrict the possible domain of validity of solution (7.4). The borderline determined by the first condition lies near the solid line in figure 2 for small γ and approaches the dashed line from below for large γ. The second edge lies entirely within region I. These observations further support the phase structure displayed in figure 2. This transition remains to be established more firmly in a future investigation, as well as the exact phase structure of the model. Furthermore, the effects of possible constraints on the correct solutions [10] should to be taken into account.

Again as in the long-range case, the small u behaviour of $\lambda_+(u)$ in all of the solutions with $\beta \neq 0$ implies that in all phases the values of β_0 and ν equal their $\gamma = 0$ values (equations (4.8) and (4.9)).

8. Discussion

In this work we have focused on directed paths in a complex random potential, which are pertinent to the study of interference effects in electron hopping through disordered materials. Application of the replica method leads to a many-body quantum system comprised of two sets of 'charged' particles, which we treat variationally. A proposed scaling relation (equation (1.2)) connects the ground-state properties of the many-body system to the wandering exponent (ν) of the directed walk.

One outcome of this investigation is that the range of correlations of the disorder has a major effect on the phase diagram of this problem. When both the real and imaginary parts have long-range correlations, we have found evidence for a transition only at $\beta = 0$ (i.e. in the absence of random amplitudes). This transition is marked not only by a modification in the pattern of replica-symmetry breaking but also by a change in exponents—the exponent ν shifts from the value of $3/2(1 + \gamma_0)$ when $\beta \neq 0$ to the value of $\frac{1}{2}$ for $\beta = 0$ and similarly for other exponents. The addition of

random phases to the problem of directed walks already incurring random amplitudes results in 'pairing' of oppositely charged replicas. This change occurs quite smoothly in the case with long-range correlations ($0 < \gamma_0 < 2$). On the other hand, in the 'mixed' case with long-range amplitude correlations and short-range phase correlations, the binding among replicas shifts abruptly, and a non-trivial phase diagram consisting of at least two and very likely three or more phases emerges. In the weak-coupling phase (small β and small γ) the imaginary part of the random potential does not play a significant role, but in the other phase(s), in particular for large γ and small β, it modifies the properties of the system. This behaviour is reminiscent of the phase transition obtained in the case of short-ranged correlations for both the real and imaginary parts of the disorder [10]. More research is necessary to obtain the exact form of the phase diagram in the mixed case. In addition, the case of random amplitudes with short-range correlations and random phases with long-range correlations remains an as yet unexplored territory.

These variational results become exact for high spatial dimensions. There remains some uncertainty concerning how they would be modified for the cases of $N = 1$ and $N = 2$, which correspond to the real systems. Solutions on the Cayley tree should in principle correspond to $N = \infty$ and complement the variational replica approach used here. Such results are available only in the short-range case [25]; extension of these solutions to the long-range and mixed cases would be helpful.

Acknowledgment

We gratefully acknowledge financial support under NSF grant DMR-9016907.

Appendix

In this appendix, we consider the $n \to 0$ limit of the hierarchical matrices introduced by Parisi [12] in the natural language of their eigenvalues. This reformulation simplifies extending the variational calculations to those involving two sets of n 'particles' as required in the study of directed walks acquiring both random amplitudes and random phases. Let $\hat{A}$ be an $n \times n$ hierarchical matrix with K-step breaking; its matrix elements are given by

$$\begin{aligned} A_{aa} &= \tilde{a} \\ A_{ab} &= a_i \qquad \text{if } I(a/m_i) \neq I(b/m_i) \text{ and } I(a/m_{i+1}) = I(b/m_{i+1}) \end{aligned} \tag{A.1}$$

where m_i $(i = 0, \ldots, K+1)$ are integers such that m_{i-1}/m_i is also an integer with $m_0 = 1$ and $m_{K+1} = n$, $I(x)$ is the smallest integer greater than or equal to x, and a_i $(i = 0, \ldots, K)$ are real numbers. Such a matrix can be expressed in the following way

$$\begin{aligned} \hat{A} = {} & (\tilde{a} - a_0)\hat{I}_{n/m_K} \otimes \hat{I}_{m_K/m_{K-1}} \otimes \cdots \otimes \hat{I}_{m_2/m_1} \otimes \hat{I}_{m_1} \\ & + (a_0 - a_1)\hat{I}_{n/m_K} \otimes \hat{I}_{m_K/m_{K-1}} \otimes \cdots \otimes \hat{I}_{m_2/m_1} \otimes \hat{J}_{m_1} \\ & + (a_1 - a_2)\hat{I}_{n/m_K} \otimes \hat{I}_{m_K/m_{K-1}} \otimes \cdots \otimes \hat{J}_{m_2/m_1} \otimes \hat{J}_{m_1} \\ & + \cdots + (a_{K-1} - a_K)\hat{I}_{n/m_K} \otimes \hat{J}_{m_K/m_{K-1}} \otimes \cdots \otimes \hat{J}_{m_2/m_1} \otimes \hat{J}_{m_1} \\ & + a_K \hat{J}_{n/m_K} \otimes \hat{J}_{m_K/m_{K-1}} \otimes \cdots \otimes \hat{J}_{m_2/m_1} \otimes \hat{J}_{m_1} \end{aligned} \tag{A.2}$$

where $\hat{I}_j$ is the $j \times j$ identity matrix, $\hat{J}_j$ is the $j \times j$ matrix with all matrix elements equaling one, and $\hat{I}_j \otimes \hat{J}_k$ denotes the matrix direct product of $\hat{I}_j$ and $\hat{J}_k$. As a step toward the eventual $n \to 0$ limit, define a piecewise continuous function $a(u)$ on the interval $[1, n]$

$$a(u) = a_i \qquad \text{if } m_i < u \leqslant m_{i+1} \tag{A.3}$$

so that $a(m_{i+1}) = a_i$.

The eigenvectors of $\hat{A}$ are the direct products of the eigenvectors of the $\hat{J}$ matrices. The eigenvectors are independent of the parameters $(\tilde{a}, a(u))$; consequently, two hierarchical matrices with the same pattern of breaking (i.e. the same m_is) commute. The eigenvalues of $\hat{A}$ and their corresponding multiplicities are

Eigenvalue	Multiplicity
$\lambda_a(m_1) = \tilde{a} - a_0$	$n(m_1 - 1)/m_1$
$\lambda_a(m_2) = \tilde{a} + (m_1 - 1)a_0 - m_1 a_1$	$n(m_2 - m_1)/m_2 m_1$
$\vdots$	$\vdots$
$\lambda_a(n) = \tilde{a} + (m_1 - 1)a_0 + \cdots + (m_K - m_{K-1})a_{K-1} - m_K a_K$	$n(n - m_k)/n m_K$
$\tilde{\lambda}_a = \tilde{a} + (m_1 - 1)a_0 + \cdots + (m_K - m_{K-1})a_{K-1} + (n - m_K)a_K$	1.

(A.4)

The eigenvalues (with the exception of $\tilde{\lambda}$) are defined as the steps of a piecewise continuous function just as with the as. Note that there are equal numbers of λs and as; hence, the parameters $(\tilde{a}, a(u))$ can be expressed in terms of the eigenvalues as follows

$$\begin{aligned}
a(n) &= \frac{1}{n}\tilde{\lambda}_a - \frac{1}{n}\lambda_a(n) \\
a(m_K) &= \frac{1}{n}\tilde{\lambda}_a + \left(\frac{1}{m_K} - \frac{1}{n}\right)\lambda_a(n) - \frac{1}{m_K}\lambda_a(m_K) \\
&\vdots \\
a(m_1) &= \frac{1}{n}\tilde{\lambda}_a + \left(\frac{1}{m_K} - \frac{1}{n}\right)\lambda_a(n) + \cdots + \left(\frac{1}{m_1} - \frac{1}{m_2}\right)\lambda_a(m_2) - \frac{1}{m_1}\lambda_a(m_1) \\
\tilde{a} &= \frac{1}{n}\tilde{\lambda}_a + \left(\frac{1}{m_K} - \frac{1}{n}\right)\lambda_a(n) + \cdots + \left(\frac{1}{m_1} - \frac{1}{m_2}\right)\lambda_a(m_2) + \left(1 - \frac{1}{m_1}\right)\lambda_a(m_1).
\end{aligned} \tag{A.5}$$

In the continuous notation, the previous relations are re-expressed as

$$\begin{aligned}
\lambda_a(u) &= \tilde{a} + \int_1^u \mathrm{d}v\, a(v) - u a(u) \\
\tilde{\lambda}_a &= \tilde{a} + \int_1^n \mathrm{d}v\, a(v)
\end{aligned} \tag{A.6}$$

and

$$\begin{aligned}
a(u) &= \frac{1}{n}\tilde{\lambda}_a + \int_u^n \frac{\mathrm{d}v}{v^2}\lambda_a(v) - \frac{1}{u}\lambda_a(u) \\
\tilde{a} &= \frac{1}{n}\tilde{\lambda}_a + \int_1^n \frac{\mathrm{d}u}{u^2}\lambda_a(u).
\end{aligned} \tag{A.7}$$

The continuous notation provides the natural setting for taking the $n \to 0$ limit. (As n approaches zero, the inequality $1 \leqslant m_1 \leqslant \cdots \leqslant m_K \leqslant n$ becomes $n \leqslant m_K \leqslant \cdots \leqslant m_1 \leqslant 1$, and of course, the m_i need no longer be integers.) In this limit, Mézard and Parisi [9] introduce the notation

$$\begin{aligned} \langle a \rangle &= \int_0^1 \mathrm{d}u\, a(u) \\ [a](u) &= -\int_0^u \mathrm{d}v\, a(v) + u a(u) \end{aligned} \tag{A.8}$$

in terms of which, the eigenvalues are expressed as

$$\lambda_a(u) = \tilde{a} - \langle a \rangle - [a](u). \tag{A.9}$$

That this quantity is an eigenvalue of the hierarchical matrix explains its prevalence in their calculations [9]. Note that we will refrain from replacing n with zero, since we calculate the n-dependence of the ground-state energy in order to extract the exponent β_0.

Any quantity that can be calculated from $\hat{A}$ has a natural expression in terms of its eigenvalues. For example, if $\hat{B}$ (parametrized by $(\tilde{b}, b(u))$ is the inverse of $\hat{A}$, i.e. $\hat{B} = \hat{A}^{-1}$, then the bs are given by

$$\begin{aligned} b(u) &= \frac{1}{n}\tilde{\lambda}_a^{-1} + \int_u^n \frac{\mathrm{d}v}{v^2}\lambda_a^{-1}(v) - \frac{1}{u}\lambda_a^{-1}(u) \\ \tilde{b} &= \frac{1}{n}\tilde{\lambda}_a^{-1} + \int_1^n \frac{\mathrm{d}u}{u^2}\lambda_a^{-1}(u) \end{aligned} \tag{A.10}$$

where $\lambda_a^{-1}(u) = 1/\lambda_a(u)$. These equations are like those for $(\tilde{a}, a(u))$ only with $(\tilde{\lambda}_a, \lambda_a(u))$ replaced by $(\tilde{\lambda}_a^{-1}, \lambda_a^{-1}(u))$.

Consider now the $2n \times 2n$ matrix $\hat{M}$

$$\hat{M} = \begin{pmatrix} \hat{C} & \hat{D} \\ \hat{D} & \hat{C} \end{pmatrix} \tag{A.11}$$

where $\hat{C}$ and $\hat{D}$ are hierarchical matrices. If $\hat{C}$ and $\hat{D}$ have the same m_i, they commute. Then the eigenvectors of $\hat{M}$ are simply $\binom{1}{1} \otimes v$ and $\binom{1}{-1} \otimes v$, where v are the shared eigenvectors of $\hat{C}$ and $\hat{D}$. The corresponding eigenvalues are

$$\begin{aligned} \lambda_+(u) &= \lambda_c(u) + \lambda_d(u) & \lambda_-(u) &= \lambda_c(u) - \lambda_d(u) \\ \tilde{\lambda}_+ &= \tilde{\lambda}_c + \tilde{\lambda}_d & \tilde{\lambda}_- &= \tilde{\lambda}_c - \tilde{\lambda}_d \end{aligned} \tag{A.12}$$

in terms of the eigenvalues of the individual $n \times n$ hierarchical matrices. And in terms of these eigenvalues, cs and ds are

$$\begin{aligned} c(u) &= \frac{1}{2n}(\tilde{\lambda}_+ + \tilde{\lambda}_-) + \frac{1}{2}\int_u^n \frac{\mathrm{d}v}{v^2}(\lambda_+(v) + \lambda_-(v)) - \frac{1}{2u}(\lambda_+(u) + \lambda_-(u)) \\ \tilde{c} &= \frac{1}{2n}(\tilde{\lambda}_+ + \tilde{\lambda}_-) + \frac{1}{2}\int_1^n \frac{\mathrm{d}u}{u^2}(\lambda_+(u) + \lambda_-(u)) \\ d(u) &= \frac{1}{2n}(\tilde{\lambda}_+ - \tilde{\lambda}_-) + \frac{1}{2}\int_u^n \frac{\mathrm{d}v}{v^2}(\lambda_+(v) - \lambda_-(v)) - \frac{1}{2u}(\lambda_+(u) - \lambda_-(u)) \\ \tilde{d} &= \frac{1}{2n}(\tilde{\lambda}_+ - \tilde{\lambda}_-) + \frac{1}{2}\int_1^n \frac{\mathrm{d}u}{u^2}(\lambda_+(u) - \lambda_-(u)) \end{aligned} \tag{A.13}$$

and the parameters defining $\hat{M}^{-1}$ are obtained by replacing λs with λ^{-1}s.

References

[1] Faran O and Ovadyahu Z 1988 *Phys. Rev.* B **38** 5457
Zhang Y, Dai P and Sarachik M P 1992 *Phys. Rev.* B **45** 9473
[2] Fritzsche H and Pollak M (ed) 1990 *Hopping and Related Phenomena* (Singapore: World Scientific)
Pollak M and Shklovskii B I (ed) 1991 *Hopping Transport in Solids* (Amsterdam: North-Holland)
[3] Nguyen V L, Spivak B Z and Shklovskii B I 1985 *JETP Lett.* **41** 42; 1985 *Sov. Phys.–JETP* **62** 1021; 1986 *JETP Lett.* **43** 44
[4a] Shapir Y and Wang X R 1987 *Europhys. Lett.* **4** 1165
[4b] Entin-Wohlman O, Imry Y and Sivan U 1989 *Phys. Rev.* B **40** 8342
[5] Medina E, Kardar M, Shapir Y and Wang X R 1989 *Phys. Rev. Lett.* **62** 941
[6] Al'tshuler B L and Lee P A 1988 *Physics Today* **41** (Dec) 36
Webb R A and Washburn S 1988 *Physics Today* **41** (Dec) 46
[7] Parisi G 1990 *J. Physique* **51** 1595
Mézard M 1990 *J. Physique* **51** 1831
[8] Derrida B and Spohn H 1988 *J. Stat. Phys.* **51** 817
[9] Mézard M and Parisi G 1991 *J. Physique* I **1** 809; 1990 *J. Phys. A: Math. Gen.* **23** L1229
[10] Goldschmidt Y Y and Blum T 1992 *J. Physique* I **2** 1607
[11] Derrida B 1981 *Phys. Rev.* B **24** 2613
Gross D J and Mézard M 1984 *Nucl. Phys.* B **240** 431
[12] Mézard M, Parisi G and Virasoro M A 1987 *Spin Glass Theory and Beyond* (Singapore: World Scientific)
Binder K and Young A P 1986 *Rev. Mod. Phys.* **58** 801
[13] Shakhnovich E I and Gutin A M 1989 *J. Phys. A: Math. Gen.* **22** 1647
[14] Kardar M 1987 *Nucl. Phys.* B **290** 582
[15] Zhang Y C 1989 *Europhys. Lett.* **9** 113
[16] Huse D A and Henley C L 1985 *Phys. Rev. Lett.* **54** 2708
Kardar M and Zhang Y C 1987 *Phys. Rev. Lett.* **58** 2087
[17] Huse D A, Henley C L and Fisher D S 1985 *Phys. Rev. Lett.* **55** 2924
Medina E, Hwa T, Kardar M and Zhang Y C 1989 *Phys. Rev.* A **39** 3053
[18] Blum T and Goldschmidt Y Y 1992 Directed paths with random phases *Nucl. Phys.* B **380** 588
[19] McGuire J B 1964 *J. Math. Phys.* **5** 622
[20] Goldschmidt Y Y and Mézard M 1991 unpublished
[21] Parisi G 1990 *R. Acad. Naz. Lincei.* **XI-1** 3
[22] Nattermann T 1985 *J. Phys. C: Solid State Phys.* **18** 6661
Kardar M 1987 *J. Appl. Phys.* **61** 3601
[23] Zhang Y C 1990 *Phys. Rev.* B **42** 4897
Kolomeisky E B 1991 *Phys. Rev.* B **45** 7094
[24] Blum T, Shapir Y and Koltun D S 1991 *J. Physique* I **1** 613
[25] Cook J and Derrida B 1990 *J. Stat. Phys.* **61** 961